CONF-950793--33

Hybrid optics for the visible produced by bulk casting of sol-gel glass using diamond-turned molds

Bruce E. Bernacki, Arthur C. Miller, L. Curt Maxey, and Joseph P. Cunningham
Oak Ridge National Laboratory
P. O. Box 2009, MS 6002, Oak Ridge, Tennessee 37831-6002

William V. Moreshead and Jean-Luc R. Noguès
GELTECH, Inc.
One Progress Blvd. #8, Alachua, Florida 32615

In support of work performed by Martin Marietta Energy Systems, Inc., for the U.S. Department of Energy under contract DE-AC05-84OR21400

Hybrid optics for the visible produced by bulk casting of sol-gel glass using diamond-turned molds

Bruce E. Bernacki, Arthur C. Miller, L. Curt Maxey, and Joseph P. Cunningham

Oak Ridge National Laboratory
P. O. Box 2009, MS 6002, Oak Ridge, Tennessee 37831-6002

William V. Moreshead and Jean-Luc R. Noguès

GELTECH, Inc.
One Progress Blvd. #8, Alachua, Florida 32615

ABSTRACT

Recent combinations of diffractive and refractive functions in the same optical component allow designers additional opportunities to make systems more compact and enhance performance. This paper describes a research program for fabricating hybrid refractive/diffractive components from diamond-turned molds using the bulk casting of sol-gel silica glass. We use the complementary dispersive nature of refractive and diffractive optics to render two-color correction in a single hybrid optical element.

Since diamond turning has matured as a deterministic manufacturing technology, techniques previously suitable only in the infrared are now being applied to components used at visible wavelengths. Thus, the marriage of diamond turning and sol-gel processes offers a cost-effective method for producing highly customized and specialized optical components in high quality silica glass. With the sol-gel casting method of replication, diamond-turned mold costs can be shared over many pieces. Diamond turning takes advantage of all of the available degrees of freedom in a single hybrid optical element: aspheric surface to eliminate spherical aberration, kinoform surface for control of primary chromatic aberration, and the flexibility to place the kinoform on non-planar surfaces for maximum design flexibility. We will discuss the critical issues involved in designing the hybrid element, single point diamond-turning the mold, and fabrication in glass using the sol-gel process.

Key Words: hybrid optics, diffractive optics, diamond turning, SPDT, SPT, kinoform, optical replication, sol-gel glass

1. INTRODUCTION

Hybrid optical elements combine diffractive and refractive optical surfaces within the same element or system for enhancing performance by reducing or eliminating aberrations (both monochromatic and chromatic),[1,2] and reducing temperature effects.[3] One can combine discrete diffractive optical elements (DOEs) with refractive elements to achieve these improvements. The DOEs can be produced holographically, or by direct write methods, such as electron beam or optical lithography. Only the direct-write methods can easily produce the continuous phase surfaces capable of 100% diffraction efficiency, although others have shown[4] great ingenuity in circumventing the limitations of holographic approaches. Swanson and Veldkamp[5] recognized that integrated circuit fabrication techniques could be exploited to produce DOEs using discrete approximations of kinoforms. They showed that by using only four masks, a DOE with 16 phase levels having a theoretical diffraction efficiency of 99.0% was possible. Furthermore, these DOEs could be fabricated either as individual elements, or directly on planar surfaces of refractive optical elements. However, due to the limitations of masked-based lithography, these kinoforms cannot be produced on non-planar surfaces.

Advances in deterministic optical manufacturing, notably single point diamond turning (SPDT) provide an obvious additional method for fabricating kinoforms by directly machining the phase profiles into suitable materials. This method is embraced for infrared optics where the refractive optical materials are costly, and where SPDT is already an accepted method of manufacture for these mostly high-value systems due to the reduced scattering from tool marks at these long (3-5 μm and 8-14 μm) wavelengths.[6] However, SPDT was quickly shown capable of producing kinoforms with acceptable

quality for some applications in the visible.[7] The key limitation of SPDT for hybrid optics manufacture is the fidelity possible when using a diamond tool having a finite radius. The challenge is set by the spacing of the outermost zone of the kinoform, which is found using the approximate expression in Eq. 1[8]:

$$\Delta_{min} \approx 2\lambda F/\# \tag{1}$$

where the approximation is valid for large F/# lenses (F >> 1). A second limitation to SPDT is the limited variety of refractive materials that can be machined, especially for visible applications, where one is limited primarily to the optical plastics. Plastics are unacceptable for many demanding applications due to their large coefficient of thermal expansion (CTE), large change in index of refraction with temperature (dn/dT), poor solvent resistance, low melting point, low homogeneity (compared with optical glass), limited optical characteristics (index of refraction and dispersion), and the difficulties involved in applying optical coatings.[9] Finally, SPDT machinery is costly and and in non-defense applications its use can be justified only for high-value or specialty optics, or mold production for high-volume replication.

The combination of SPDT with monolithic sol-gel replication methods offers the promise of practical and cost-effective production of hybrid optics for the visible. SPDT can fabricate aspheric surfaces and kinoforms on non-planar base surfaces. Monolithic sol-gel casting makes available one of the best optical materials, silica, with its broad transmission characteristic, low CTE and dn/dT, high homogeneity and purity, high melting point and resistance to water and solvents, and high tolerance to ionizing radiation effects. SPDT forms can be used to produce injection molds for casting the sol-gel optics to share the cost of producing the mold form over many copies. Due to the variety of optical surfaces made available to the optical designer through SPDT, the hybrid approach is best used solely to achromatize the lens or system, which results in relatively slow surfaces having few zones,[10] relaxing fabrication demands. Finally, there is significant isotropic shrinkage inherent in the sol-gel replication process (a factor of 2.5) that applies to the tool marks from the SPDT mold, essentially extending the applicability of SPDT into the visible regime. The design, fabrication, and performance of a hybrid singlet replicated using sol-gel casting is presented in detail below.

2. DESIGN OF THE HYBRID LENS

2.1 Cast Optic Design

The first order design of hybrid refractive/diffractive elements is well documented in the literature, and the analytic approach will not be followed here. Essentially, the identical approach to traditional achromatic design is followed with the substitution of a diffractive Abbe number (reciprocal dispersion) for the kinoform element. Stone and George [Ref. 2] provide an accessible and well-written account of the analytic hybrid design approach. The diffractive Abbe number v_D of -3.45 common to all diffractive elements holds to key to achromatic design using a single glass type: it is negative and has a relatively small magnitude, unlike the positive Abbe numbers for all optical glasses, whose reciprocal dispersions are an order of magnitude greater (are much less dispersive). Therefore, a weak diffractive surface can be found that can be made to bring two wavelengths of light to a common focus. Unlike the usual achromat that has positive and negative elements, the hybrid singlet's surfaces both have positive power, with focal lengths greater than the focal length of the lens under design. Due to the large dispersive behavior of the diffractive surface, very little optical power is needed to achieve achromatization, which makes fabrication much less difficult than is required for a purely diffractive element having the same F/# as the hybrid singlet design example.

The design freedom made possible by SPDT makes analytic design approaches unwieldy, necessitating the use of automatic lens design software for optimum performance. Most commercial software allows design with holographic or binary optical elements, and even hybrid elements, in some instances. The design strategy is to first optimize the design *without using the diffractive surface* until no further improvement is noted using all of the available degrees of freedom offered by SPDT. Only then is the diffractive or binary surface implemented, which limits its use solely to achromatize the optic. Failure to observe this caveat will cause the optimization function to use the DOE to help correct the residual monochromatic aberrations, and the resulting design will exhibit excessive wavelength-sensitive aberrations. Using this approach, the design that resulted is shown in Table I. The design was constrained to a plano-convex shape due to limitations in generic molding fixtures that were readily available. The diffractive element is placed on the aspheric surface. A rotationally-symmetric polynomial was used to define the sag of the surface. The sag has the following form:

$$z = \sum_i a_i \cdot \rho^{2i} . \tag{2}$$

The coordinate system used for the lens design is based on a right-handed Cartesian system in which light propagates along the optical axis in the +Z direction. Only four terms were required to optimize the hybrid. Ray fan and longitudinal aberration plots are shown in Figure 1. The longitudinal aberration shows the large secondary spectrum inherent in hybrid designs (compared with all-glass designs) due to the highly dispersive diffractive surface. Wood[10] shows that the secondary spectrum results in a focal length variation that is expressed by:

$$df = -f \frac{(P_r - P_d)}{(\upsilon_r - \upsilon_d)} \tag{3}$$

where P_r and P_d are the partial dispersions for the refractive (0.3101) and diffractive (0.4038) surfaces, respectively, and the v_r and v_d refer to the refractive (67.8) and diffractive (-3.45) Abbe numbers. The example has a nominal 42 mm focal length, leading to a prediction of a 55 μm shift in focal length, which agrees nicely with the 60 μm shown in Figure 1(b).

Table I. Design summary of SPDT hybrid singlet.

F/#	3.3
Diameter	12.7 mm
Middle, Short and Long Design Wavelengths	0.58756 μm, 0.4861 μm, and 0.65627 μm
a_1	0.0246224
a_2	$3.632985\ 10^{-6}$
a_3	$1.326958\ 10^{-7}$
a_4	$-1.59403\ 10^{-9}$
α_1	$-5.89651\ 10^{-4}$
Material	Gelsil®(silica glass)
Index of Refraction at 0.58756 μm	1.458

The DOE is typically realized in lens design software using a phase polynomial of the form:

$$\Phi = \frac{2\pi}{\lambda_0} \cdot \sum_i \alpha_i \rho^{2i} \tag{4}$$

where λ_0 is the design wavelength, and ρ is the radial coordinate. At infinite conjugates, the relative phase at the image plane due to a DOE having focal length f_D can be expressed as:

$$\Phi = \frac{2\pi}{\lambda_0}\left(f_D - \sqrt{f_D^2 + \rho^2}\right) \tag{5}$$

and if Eq. 5 is expanded into an infinite series the result is:

$$\Phi = \frac{2\pi}{\lambda_0}\left[-\frac{\rho^2}{2f_D} + \frac{\rho^4}{8f_D^3} - \frac{\rho^6}{16f_D^5} + \frac{\rho^8}{128f_D^7} - \cdots\right]. \tag{6}$$

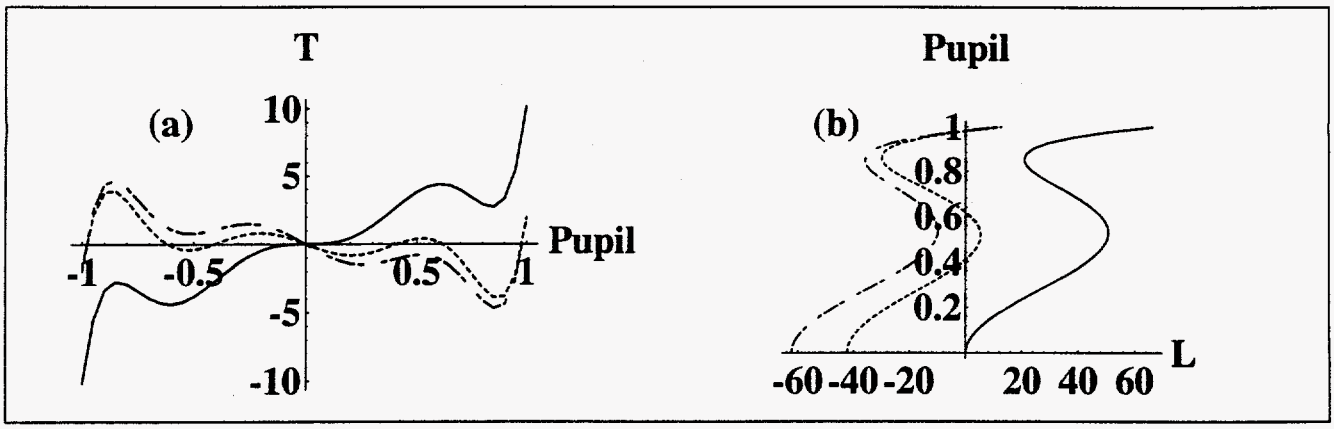

Figure 1. Ray fan plot (a) showing transverse ray deviations at the image plane in units of micrometers versus the normalized pupil coordinate. The middle (solid), short (dotted) and long (dashed-dotted) design wavelengths are depicted. Only the tangential section is shown (YZ plane) since the sagittal plot is identical. The longitudinal aberration plot in (b) for the three design wavelengths highlights the secondary spectrum inherent in hybrid achromats. Units along the optical axis are in micrometers.

Equating coefficients between Eq. 4 and Eq. 6, the effective focal length of a diffractive surface found by the automated lens design program can be calculated.[11] For this example, f_D is 848 mm resulting in an F/67 surface! Since the refractive asphere is used to minimize the monochromatic aberrations, only the first term is necessary for the diffractive phase function, as the design is comfortably within the paraxial regime with an F/# of this magnitude.

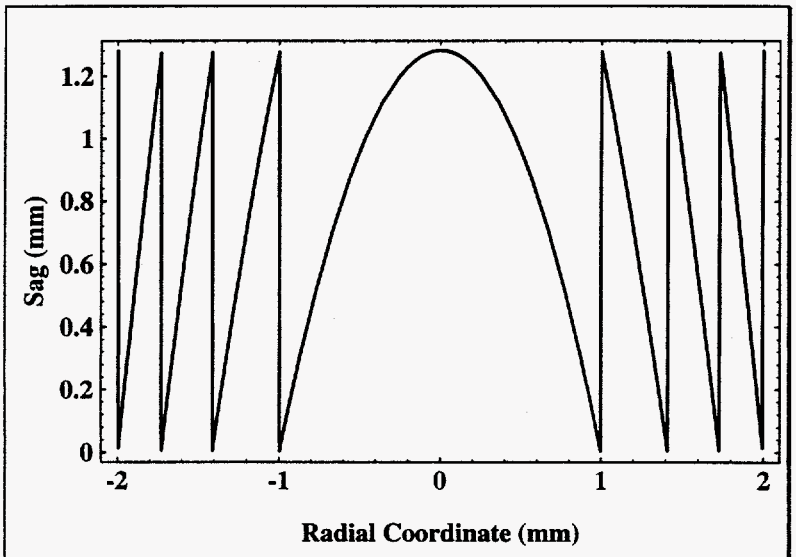

Figure 2. First several zones of the kinoform found to realize the phase function that results from the lens design calculations.

Once the phase function is determined by the lens design program, a real kinoform surface that will be fabricated using SPDT must be designed that imparts the identical phase shift found through optimization. The design phase shift is a combination of that due to the kinoform surface and its base surface. To find the base surface one solves the following phase continuity equation [Ref. 3] using the sag equations for the base and kinoform surface to determine the parent surface of the kinoform, $z_{kinoform}$:

$$-(n-1)\cdot\left(z_{base}-z_{kinoform}\right)\cdot\cos\left[\tan^{-1}\left(\frac{dz_{base}}{d\rho}\right)\right]=\alpha_1\rho^2. \tag{7}$$

The zone locations are found by finding the isophase radii modulo[2π]:

$$\frac{2\pi}{\lambda_0}\left[\alpha_1\rho^2\right]=2k\pi \tag{8}$$

and this expression can be used to plot the first few zones of the kinoform that would bring about the same phase distribution as that found through the lens design program, seen in Figure 2 for the case of a planar substrate at infinite conjugates. Equation 8 can be solved for the zone locations and maximum number of zones, and these results used to find the minimum zone spacing at the outer zone of the optic:

$$\rho_k=\sqrt{\frac{\lambda_0}{\alpha_1}k}=\rho_1\sqrt{k} \tag{9}$$

$$k_{\max}=\frac{\alpha_1 D^2}{4\lambda_0}$$

$$\Delta_{\min}=\rho_{\max}\left[1-\sqrt{1-\frac{\lambda_0}{\alpha_1\rho_{\max}^2}}\right]\approx\frac{\lambda_0}{\alpha_1 D}$$

where D is the diameter of the optic, ρ_k is the radius for each integral zone number, ρ_{max} is the radius of the optic, and k_{max} is the maximum number of kinoform zones. For this design example, the first zone is found 0.998 mm from the optical axis, and 41 zones are required to describe the kinoform surface. The minimum zone spacing is 78.5 μm. The depth of each zone, d, is maximum at the zone transition boundary and for a surface in air, is found with the following expression:

$$d=\frac{\lambda_0}{n-1}. \tag{10}$$

For silica, the depth d is 1.28 μm

2.2 Scaled Mold Design

Because of significant shrinkage on the sol-gel molding process, the desired optical design must be scaled up to compensate for this shrinkage. If the sag of the desired function is described using ordered pairs (ρ,z), then the scaled sag (using the same parameters of curvature, conic constant, and polynomial coefficients) will have coordinates (ρ/s, z/s), where s is the scale factor. The scaled general aspheric sag equation expressed in terms of scaled parameters can then be expressed as:

$$z_{scaled}=\frac{C'\rho^2}{1+\sqrt{1-(1+\kappa)C'^2\rho^2}}+\sum_i a_i'\rho^{2i} \tag{11}$$

$$C'=\frac{C}{s}$$

$$a_i'=\frac{a_i}{s^{2i-1}}$$

where C is the curvature of the base sphere, κ is the conic constant, and s is the scale factor. In the example design, the scaling of the polynomial coefficients is done using the prescription given in Eq. 11 for the a_i, as well as for the sag of the parent surface of the kinoform, $z_{kinoform}$. The locations of the zones in the scaled design, however, are calculated using the original design dimensions. The zone radii and depth are simply scaled by a factor of 2.5. The first two zones of the scaled hybrid design with the kinoform placed on the aspheric surface is depicted in Figure 3. Machining the kinoform into the

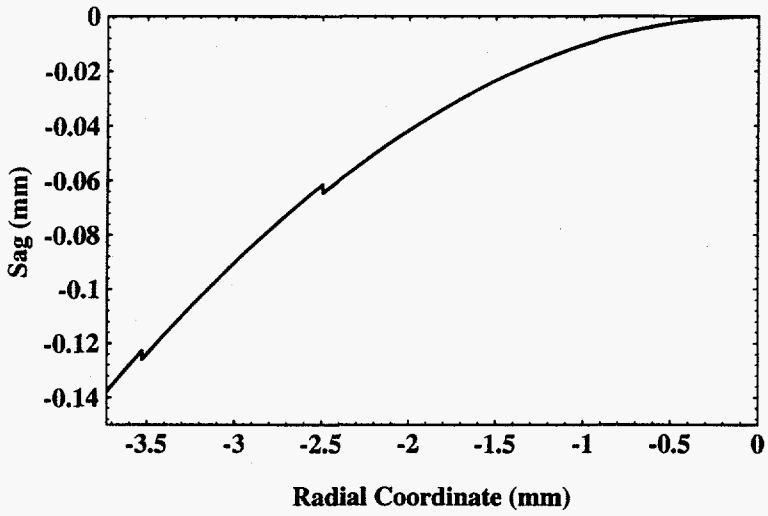

Figure 3. First two zones of the scaled hybrid design showing the kinoform placed on the aspheric surface.

aspheric surface presents some challenges to fabrication, which are detailed in the next section.

3. FABRICATION BY SINGLE POINT DIAMOND TURNING

Fabrication using SPDT usually must be justified either to achieve an optical function unattainable by other means, or when its high initial cost can be shared over many copies through replication. Several replication strategies can be followed, and are shown schematically in Figure 4. An optical element can be copied using compression molding or electro-forming, and this negative copy can be used to cast the optic, or the negative impression can be machined directly, and then cast. Our approach is to machine a mold pin in the shape of the scaled optical surface, and then to use this form to injection mold negative copies of the active surface. This disposable mold can be quite inexpensive in quantity, and does not react with the caustic sol.

The challenge to SPDT is to fabricate the sharp phase steps and kinoform facets accurately at each transition zone with regard to profile and depth. The small but finite radius of a typical diamond tool causes a fillet to be formed at each transition that would have to be cleaned up with a chisel point or "dead sharp" tool, which may do more harm to the optic and increases fabrication time. The effect of this fillet or annulus caused by the diamond tool has been termed energy blockage[12] since it does not contribute image formation. Half radius tools are available commercially[13] that facilitate the process, but still result in some minor filleting and overcutting. Also, half radius tools result in four times the peak-to-valley (PV) surface roughness than is predicted due to full radius tools for the same feed per revolution. The well-known theoretical surface finish equation for full radius tools is:

$$PV = \frac{f_F^2}{8R_T} \tag{12}$$

where f_F is the feed per revolution of the full radius tool, and R_T is the radius of the tool nose.[14] For a half radius tool, it can

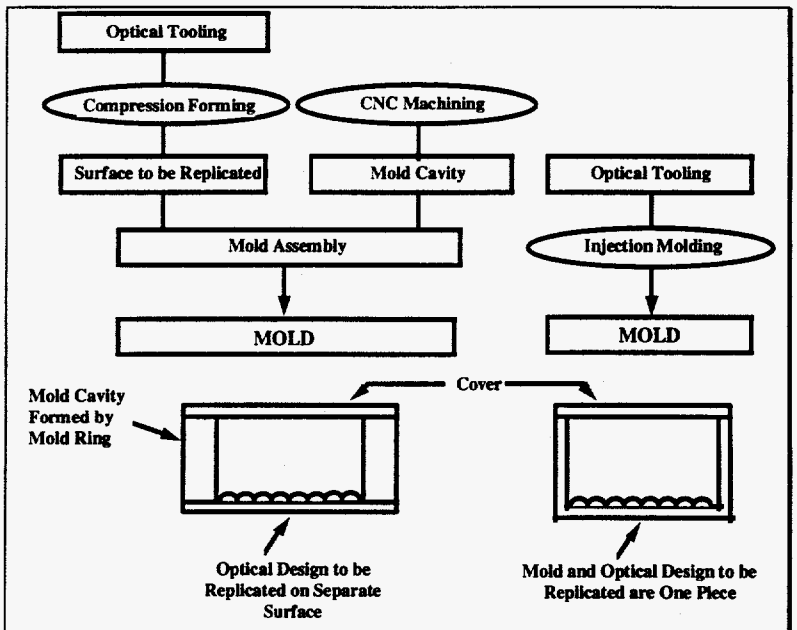

Figure 4. Common molding strategies used for replication of optical elements.

be shown that the theoretical finish equation is:

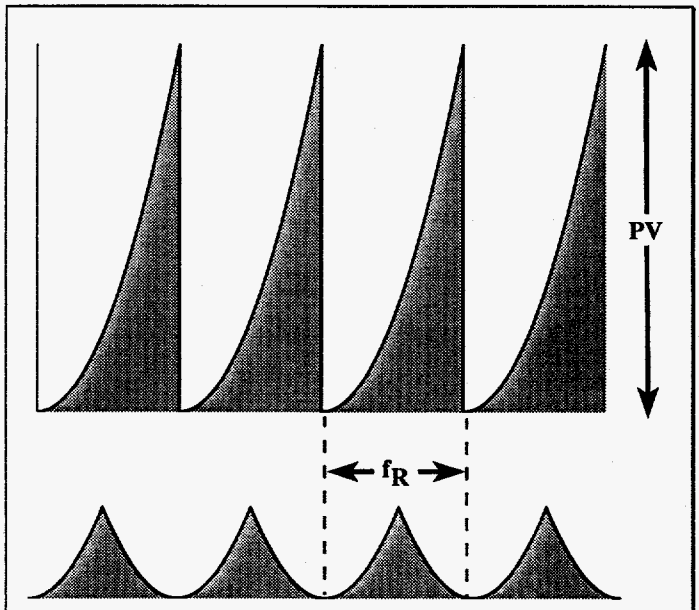

Figure 5. Tool marks due to the half radius tool (top) and a full radius tool (bottom) showing the tool advance as a function of feed rate per revolution and PV roughness. Tool marks are plotted to the same scale for identical feeds per revolution (f_R).

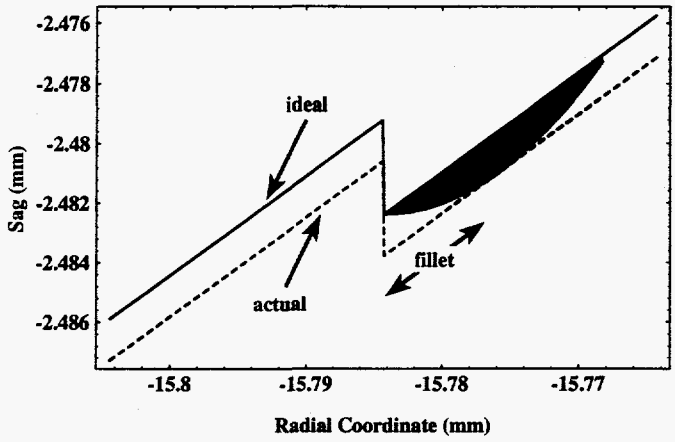

Figure 6. Transition at zone 40 showing desired tool path (solid line) along with actual tool path (dotted line). The tool outline is drawn to scale to show the fillet that results at the zone transition.

$$PV = \frac{f_H^2}{2R_T} \tag{13}$$

where f_H is the feed per revolution for the half radius tool. Equating Eq. 12 with Eq. 13, twice the feed per revolution can be used for a full radius tool to achieve the same PV surface roughness as that resulting from the half radius tool. The unique surface structure that obtains from this tool is shown in Figure 5. Use of the half radius tool greatly reduces the effects of filleting and energy blockage, although increased surface roughness can result without increased cutting times (decreased feed per revolution). Due to the local slope of the base surface combined with the slope of the kinoform that is at most pronounced at the edge of the optical element, some overcutting occurs as well as some filleting. However, as the tool approaches the center of the optic, the overcutting and filleting tends toward zero. Tool compensation algorithms can be applied to account for the tool radius and local slope, and is normally accomplished with commercial software provided with SPDT machines. No tool compensation was used for this proof-of-concept work, since the change in surface figure without tool compensation was calculated and found to be minor and could be compensated for by a change in focus. Figure 6 shows the worst-case overcutting the occurs at the outermost zone of the kinoform, as well as the unavoidable fillet. At the transition of the outermost zone, the peak height of the fillet is 1.4 μm, making the depth at the transition boundary 1.8 μm instead of 3.2 μm. Filleting also diminishes towards the center of the element. This unavoidable imperfection must be kept in perspective, since the fillet extends only 8.6 μm into the (scaled) 40th zone having a width of 198.6 μm. Therefore, for the worst-case outermost zone, only 4.3% of the kinoform facet is effected.

4. MONOLITHIC SOL-GEL CASTING

4.1 Basic Theory

Sol-gel science cannot be treated in depth here, and the reader is directed to many of the fine review articles, such as Yamane.[15] The sol-gel process can be divided into three main steps:[16] 1) gel formation, 2) drying, and 3) consolidation (densification, sintering). The sol-gel process begins with the hydrolysis and polycondensation of a silicon alkoxide, and results in the formation of a three-dimensional silica network. The net equation is summarized below:

$$Si(OR)_4 + 2H_2O \rightarrow SiO_2 + 4ROH \tag{14}$$

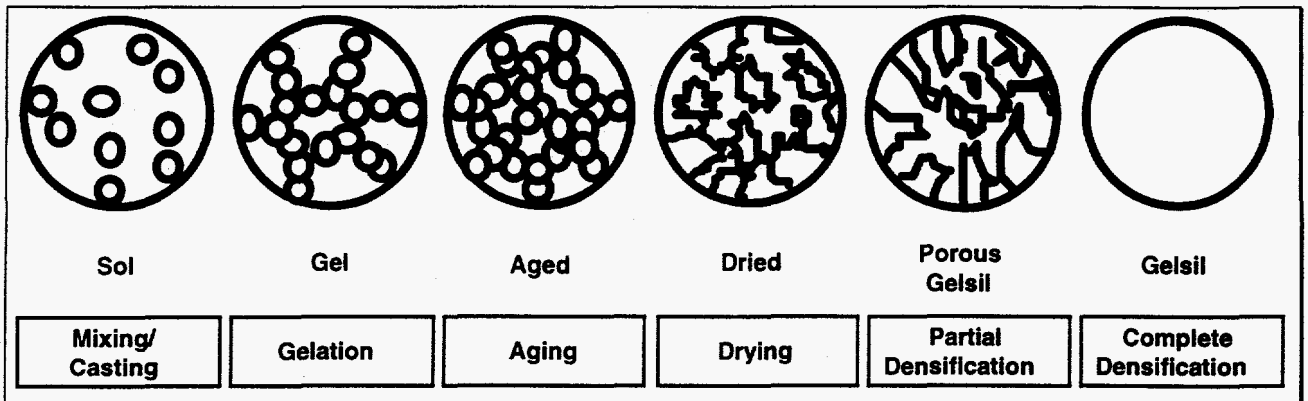

Figure 7. Schematic diagram showing the various processing steps required to produce fully dense silica (Gelsil®) using the sol-gel process.

where R is either CH_3 or C_2H_5. The liquid sol is poured into polycarbonate molds produced by injection molding of the SPDT mold pin, where it sets into a stiff gel ("wet gel"), and then is aged to increase its strength. The casting is removed from the mold and subsequently dried. This crucial step consists of eliminating the interstitial liquid from the gel body. The dried gel is heat treated to produce either a porous or dense Gelsil®. A schematic overview of the various processing steps is shown in Figure 7. The results of the monolithic casting are presented in the next section.

4.2 Replicated Hybrid Singlet

The lens prescription was scaled up by a factor of 2.5 and the surface sag, including the kinoform profile was converted into a tool path description for the SPDT machine so that a stainless steel mold pin having the same shape as the active surface could be fabricated. Approximately 4-6 mils of electroless nickel was deposited on the end of the mold pin to permit SPDT into the surface. The resulting mold pin was then used to injection mold negative impression copies of the active surface so that the sol-gel hybrid lenses could be cast. Finally, the polycarbonate molds were filled with sol and allowed to dry and age as described above. A synopsis of the results from each stage of fabrication is shown in Figure 8. A region near the edge of the mold pin, injection mold, and Gelsil® hybrid lens was probed with an optical surface profiler.

5. CONCLUSION

To our knowledge, this proof-of-concept work shows the design and fabrication of the first hybrid singlet fabricated by monolithic sol-gel casting from SPDT molds.

The improvement in the technology of deterministic optics fabrication, especially SPDT, now makes possible hybrid optical elements having aspheric shapes combined with diffractive surfaces that are suitable for many uses in the visible portion of the electromagnetic spectrum. Hybrid optics are extremely useful where the variety of refractive materials that can be diamond turned are limited, since achromatization can be achieved using a single type of optical material, and when compact, light weight, pre-aligned, robust, and low cost elements are desired. Until now, the choice was limited to the optical plastics, which are unsuitable for some applications. This is due to the sensitivity of optical plastics to changes in temperature (both CTE and dn/dT), their poor resistance to solvents and acids, poor homogeneity, and limited transmission bandwidth. Also, SPDT is perceived as expensive and its use can usually only be justified for one-of-a-kind IR defense and space systems, or in mold production for plastic optics where the replication of many elements can defray the cost of one-time mold fabrication. Monolithic sol-gel casting of refractive/diffractive hybrid optical elements addresses the lack of a high-quality optical material in SPDT optics, as well as the high cost of SPDT fabrication, by permitting the manufacturing of hybrid optical elements having aspheric surfaces and kinoforms in high-quality silica glass and sharing the cost of SPDT mold fabrication over many copies. The large isotropic shrinkage that occurs during casting also lessens the effects of SPDT tool marks, extending the use of SPDT in the fabrication of optics for visible bandwidth applications. Gelsil®, a water-free silica glass, has the advantages of low CTE and dn/dT, high melting point, excellent homogeneity, broad transmission band from 200 nm to 3.2 μm wavelength, and high resistance to damage by ionizing radiation.

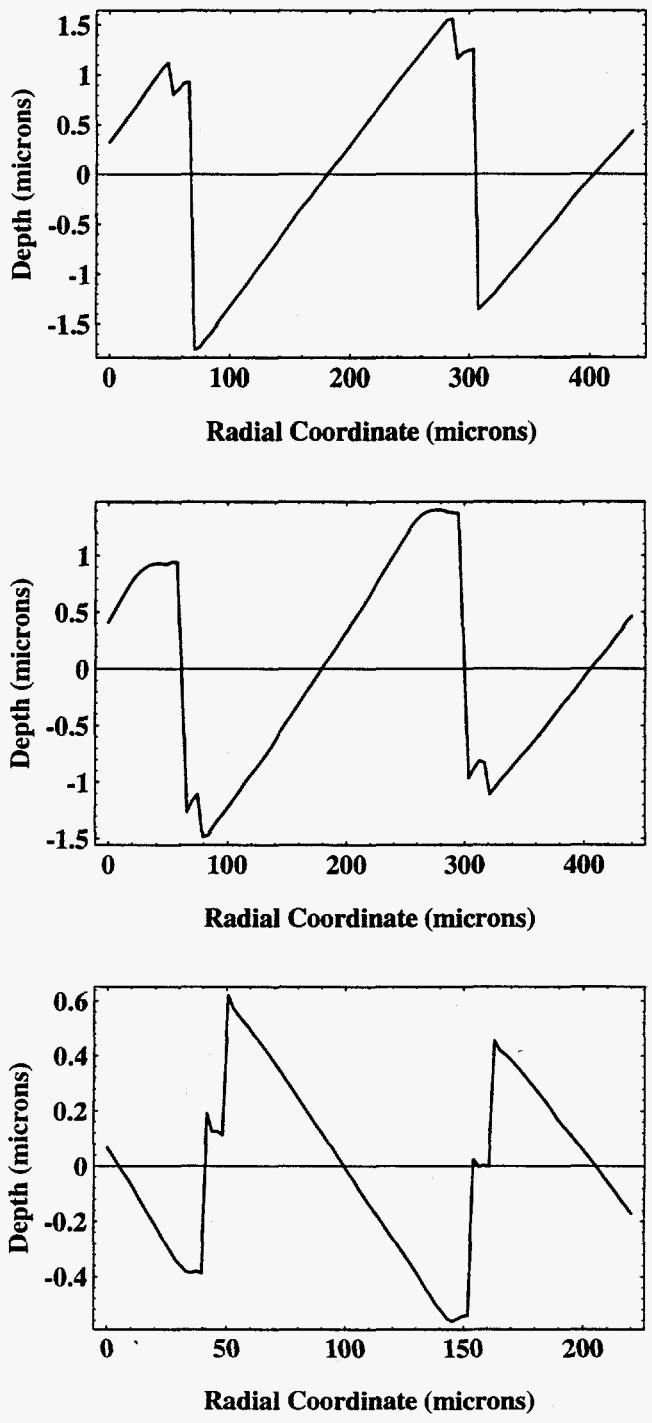

Figure 8. Cross sectional traces taken with an optical surface profiler showing kinoform facets near the edge of the mold pin (top), polycarbonate injection mold (center), and Gelsil® hybrid singlet (bottom). The sag of the base surface has been removed to highlight the kinoform facet details. Lateral resolution for the mold pin and injection mold traces was 4.4 μm/sample, while that for the Gelsil® lens was 2.2 μm/sample.

6. ACKNOWLEDGMENT

This research was done in support of work performed by Lockheed Martin Energy Systems, Inc. for the U.S. Department of Energy under contract DE-AC05-84OR21400. Funding was provided by the U.S. Army to Geltech, Inc. through the Small Business Technology Transfer (STTR) Program under contract DAAH04-94-C-0061. The authors gratefully acknowledge the encouragement and support of Dr. Jack Kruger, Chief, Target Acquisition Technology of the U.S. Army Research Office in Research Triangle Park, NC. The authors also thank Dr. Bing Fu Zhu and Mr. Layne Howell of Geltech, Inc. who made possible the fabrication of the Gelsil® lenses and optical profilometer characterization traces, and Mr. Troy Marlar of Lockheed Martin Energy Systems for his contributions in fabricating the mold pin.

7. REFERENCES

[1] Madijidi-Zolbanine, H. and C. Froehly, "Holographic correction of both chromatic and spherical aberrations of single glass lenses," *Appl. Opt.*, **18** (14), 2385-2393 (1979).

[2] Stone, T. and N. George, "Hybrid diffractive-refractive lenses and achromats," *Appl. Opt.*, **27** (14), 2960-2971 (1988).

[3] Londoño, C. W., T. Plummer, and P. P. Clark, "Athermalization of a single-component lens with diffractive optics," *Appl. Opt.*, **32** (13), 2295-2301 (1993).

[4] Hutley, M. C., R. F. Stevens, and S. J. Wilson, "The manufacture of blazed zone plates using a Fabry-Perot interferometer," *J. Mod. Opt.* **35** (2), 265-280 (1988).

[5] Swanson, G. J. and W. B. Veldkamp, "Diffractive optical elements for use in infrared systems," *Opt. Eng.* **28** (6), 605-608 (1989).

[6] Riedl, M. J. and J. T. McCann, "Analysis and performance limits of diamond turned diffractive lenses for the 3-5 and 8-12 micrometer regions," *Infrared Optical Design and Fabrication*, R. Hartmann and W. J. Smith, ed. **CR38,** 153-163 (SPIE Optical Engineering Press, Bellingham, WA, 1991)

[7] Clark, P. P. and C. Londoño, "Production of kinoforms by single point diamond machining," *Opt. Phot. News* **15** (12), 39-40 (1989).

[8] Nishihara, H. and T. Suhara, "Micro Fresnel Lenses," Chap. 1, *Progress in Optics*, **(24)** , E. Wolf, ed. (Elsevier, Amsterdam, 1987).

[9] Musikant, S., *Optical Materials*, Chap. 6 (Marcel Dekker, New York, 1985).

[10] Wood, A. P., "Design of infrared hybrid refractive-diffractive lenses," *Appl. Opt.* **31** (13), 2253-2258 (1992).

[11] ZEMAX-EE, Version 4.0, Focus Software, Inc., P. O. Box 18228, Tucson, AZ 85731

[12] Riedl, M. J., "Predesign of diamond turned refractive/diffractive elements for IR objectives," *Lens Design*, W. J. Smith, ed., **CR41,** (SPIE Optical Engineering Press, Bellingham, WA, 1992).

[13] Contour Fine Tooling, Inc., 80 Homestead Highway, North Swanzey, NH 03431.

[14] Sanger, G. M., "The precision machining of optics," Chap. 6, *Applied Optics and Optical Engineering*, R. R. Shannon and J. C. Wyant, eds., Vol 10, (Academic Press, San Diego, 1987).

[15] Yamane, M., "Monolith formation from the sol-gel process," Chap. 10, *Sol-Gel Technology for Thin Films, Fibers, Preforms, Electronics, and Speciality Shapes*, L. C. Klein, ed., (Noyes Publications, Park Ridge, NJ, 1988).

[16] Moreshead, W., B. F. Zhu, L. Howell, and J-L. Noguès, "Development of a replication process for the cost-effective manufacture of micro-optical components," presented at the *Conference on Manufacturing and Process Development in Photonics*, 1-2 November, 1994, Redstone Arsenal, Huntsville, AL.